EGU General Assembly 2020
Online | 4–8 May 2020

UNIVERSITÀ DEGLI STUDI DI MILANO BICOCCA

QUANTITATIVE FRACTURE CHARACTERIZATION IN THE DAMAGE ZONE OF THE VICTORIA FAULT, MALTA

Authors : Anna LOSA, Andrea BISTACCHI and Mattia MARTINELLI

Main goals of the project

Digital Outcrop Model (DOM)

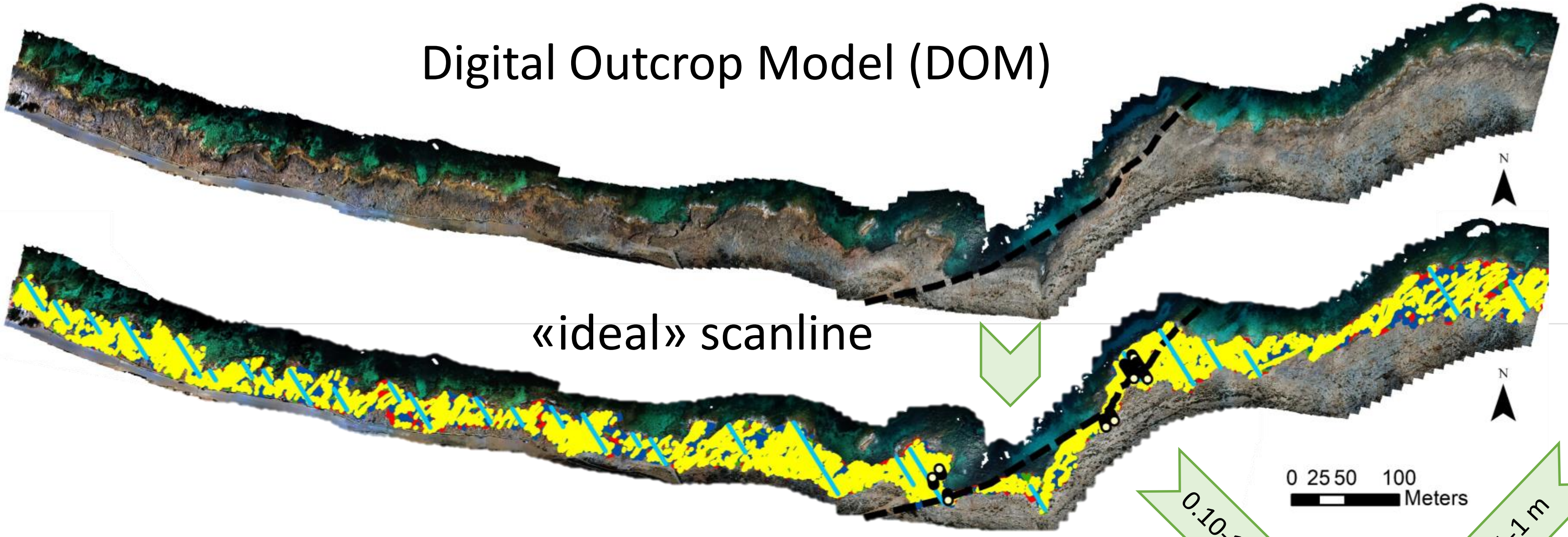

«ideal» scanline

structural analysis in the field

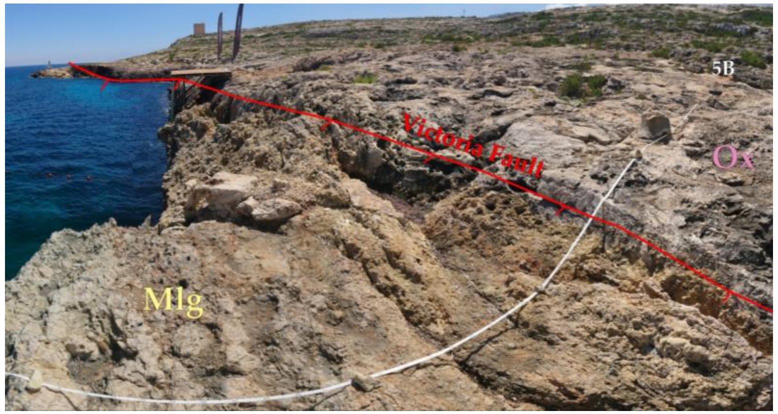

0.10-130 m

0.01-1 m

data analysis

statistical analysis

different scale

does it affect the results?

Matlab code

fracture «maturity»

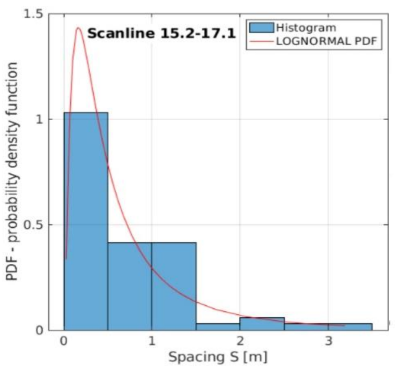

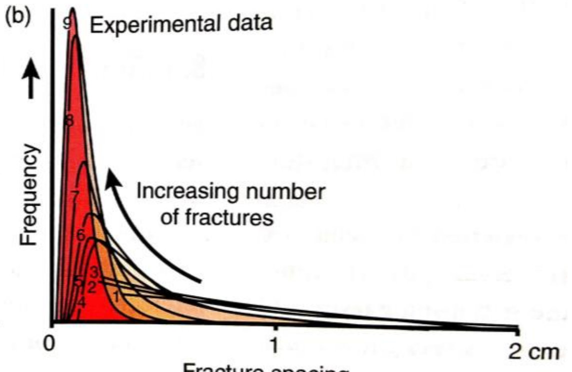

Fossen (2016)

barcode and P_{10} plot of the damage zone

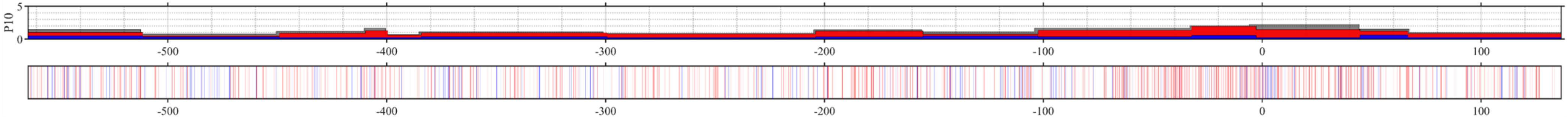

Geological framework

- Pelagian platform: foreland of the Appennine-Sicilian-Maghrebian belt
- Two main **extensional events**:
  - **D1**: WNW-ESE extension (20-17 Ma): normal fault and Neptunian dikes,
  - **D2**: N-S extension (7-1.5 Ma) and formation of the coeval sets ENE-WSW and WNW-ESE.

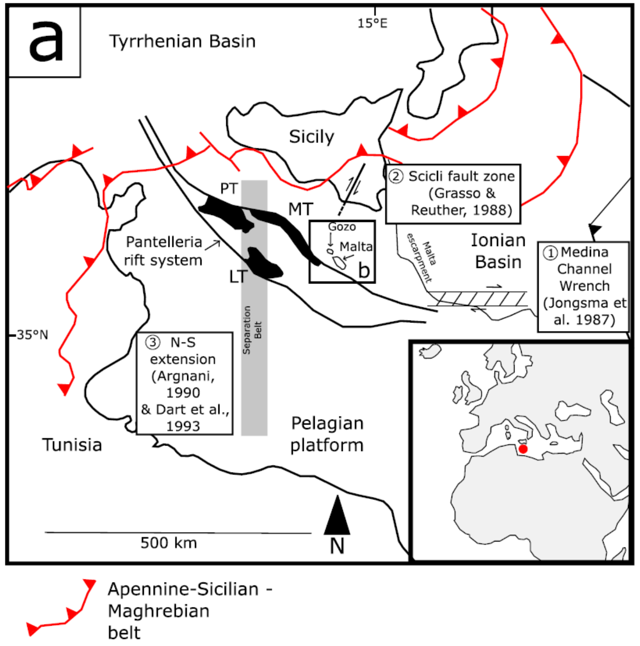

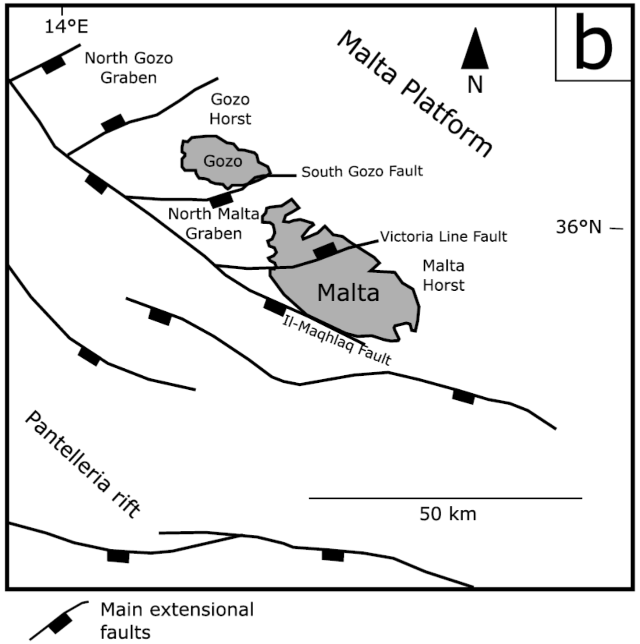

D2

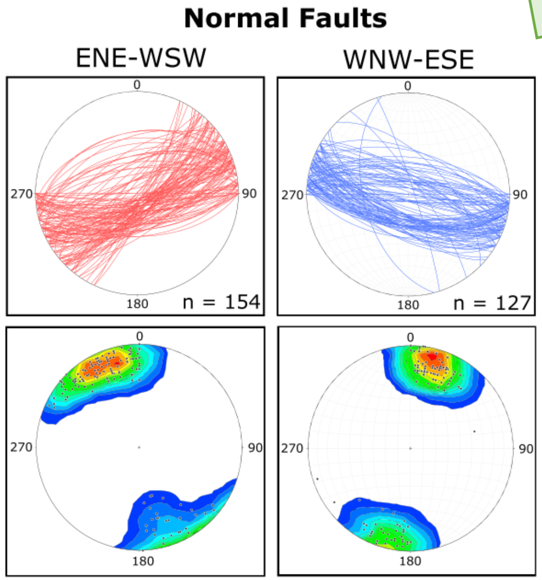

4 sets of fracture

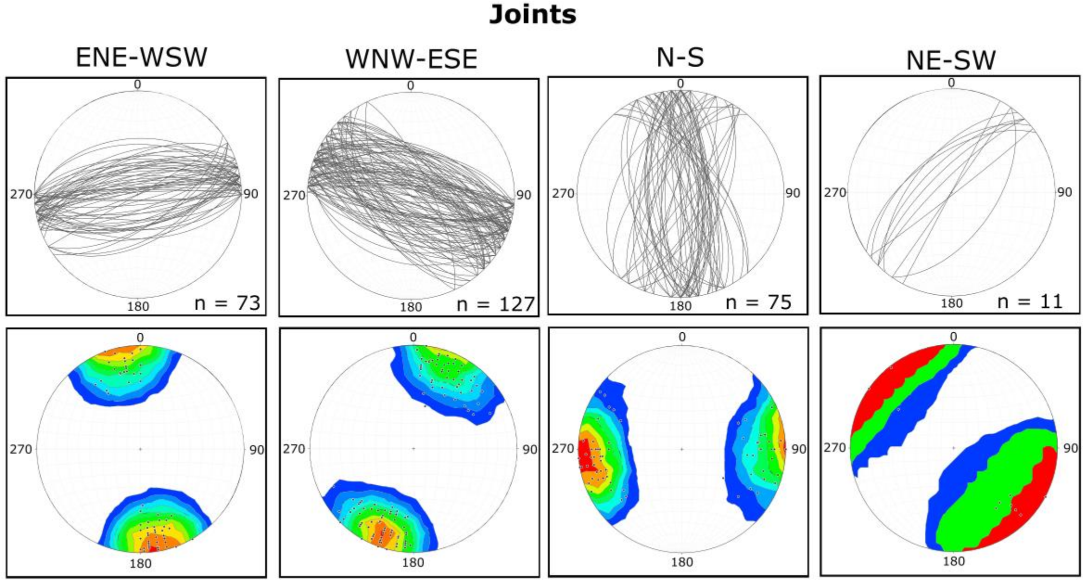

More details in Martinelli, Bistacchi, Balsamo & Meda, JSG, 2019

Stratigraphy

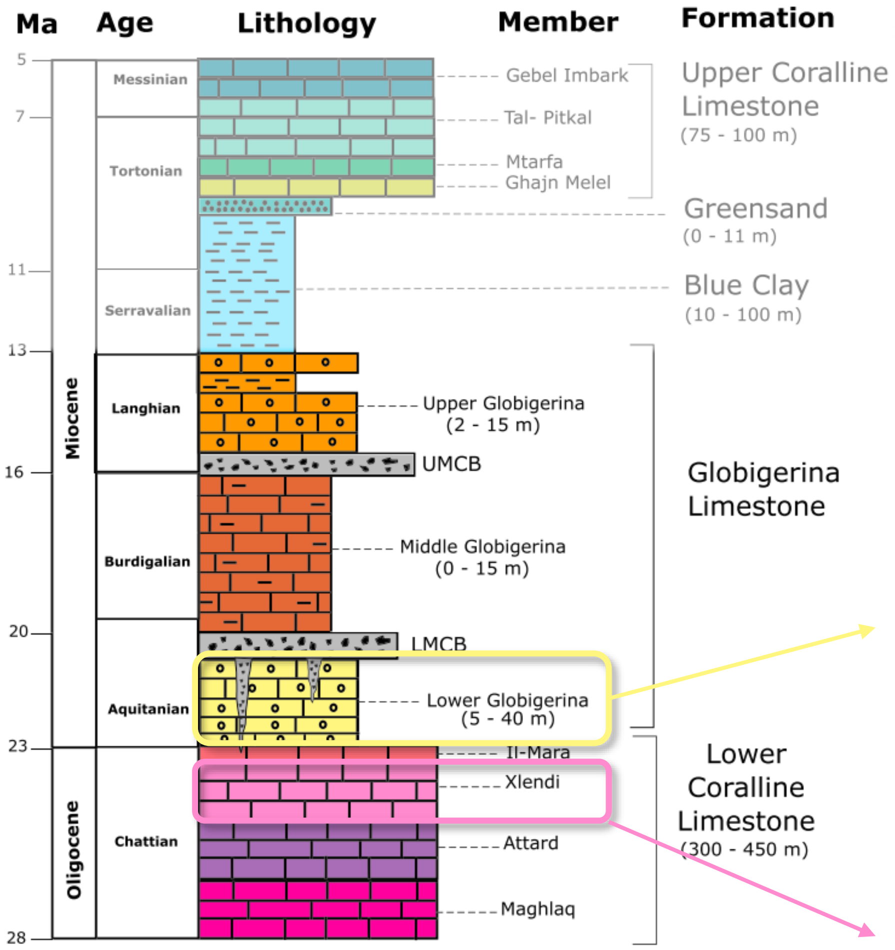

More details in Martinelli, Bistacchi, Balsamo & Meda, JSG, 2019

Lower Globigerina (Mlg): Planktonic foraminifers *Globigerina* with Neptunian dikes

Xlendi (Ox): limestones with a top layer of echinoids *Scutella subrotunda* (called *Scutella Bed*),

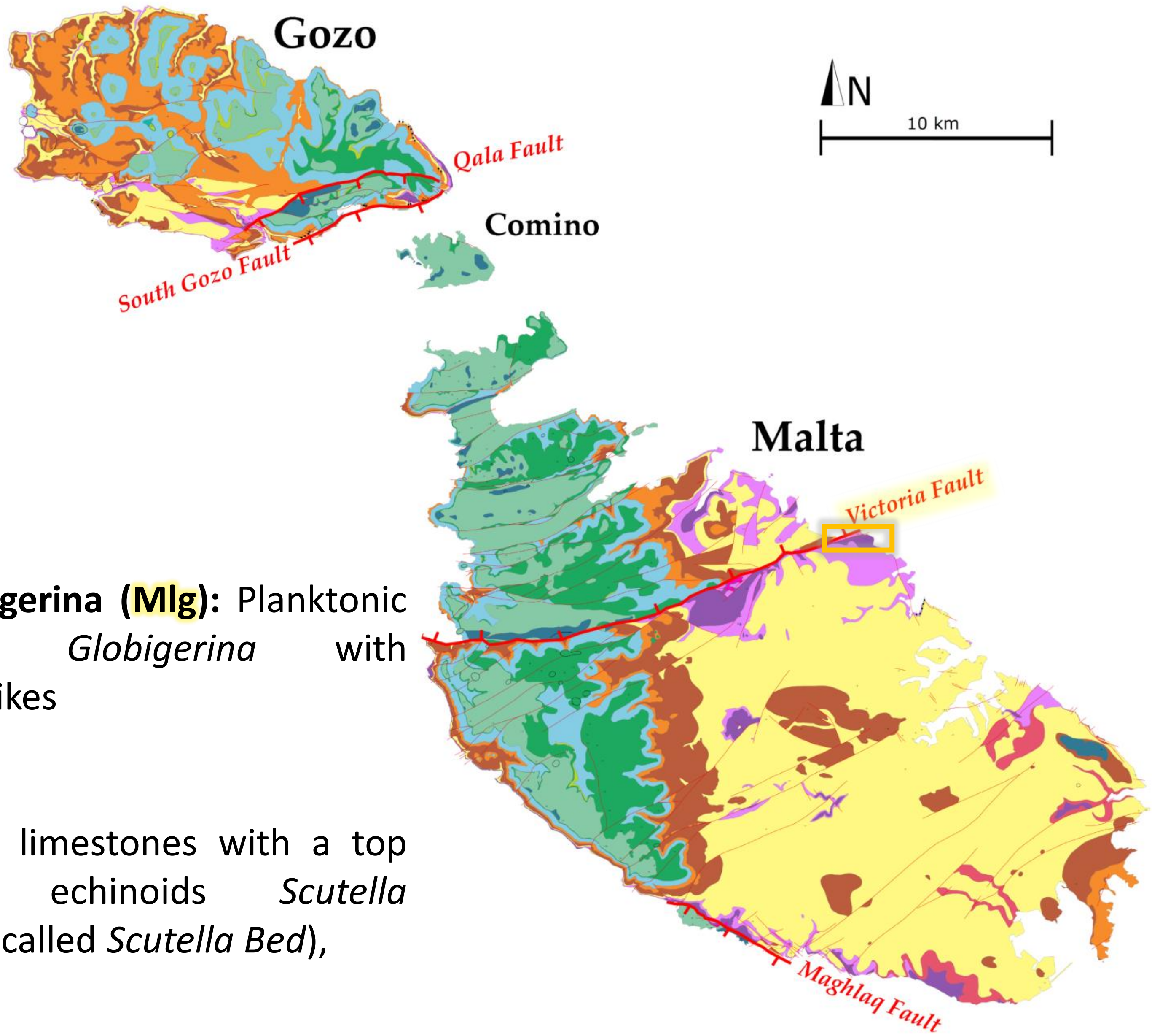

Field analysis and drone photogrammetry

PHASE 1 — FIELD ANALYSIS

- 1.1 Definition of **7 scanlines perpendicular** to the **Victoria Fault**
- 1.2 Collect data: attitude of the discontinuities, openings and filling
- 1.3 Orientation and kinematic analysis

PHASE 2 — DRONE PHOTOGRAMMETRY

- 2.1 Image acquisition (drone)
- 2.2 Photo alignment
- 2.3 Sparse and Dense point cloud
- 2.3 3D Mesh and texture building → 2.4 DTM → 2.5 Orthophoto

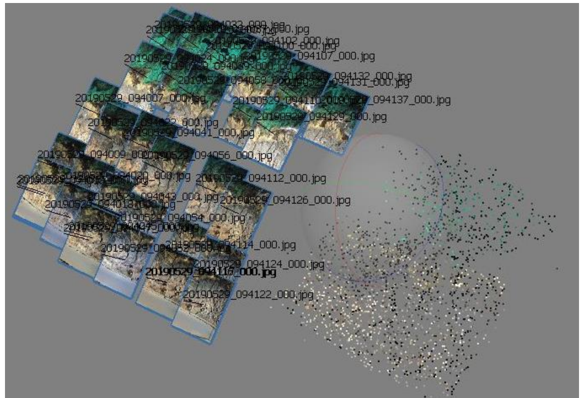
Sparse point cloud

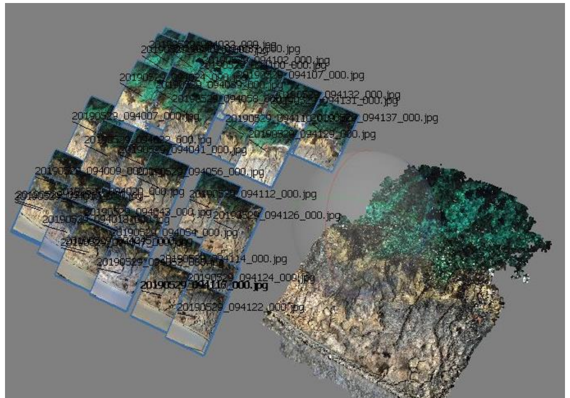
Dense point cloud

Victoria Fault NE (1)

- The 4 sets of fractures, the Victoria Fault and the lithologies were traced on the orthophotos.
- Construction of an «**ideal**» **scanline** (Azimuth 122°), segmented, and perpendicular to the Victoria Fault (Azimut 212):

main — 24 scanlines

secondary — 4 scanlines

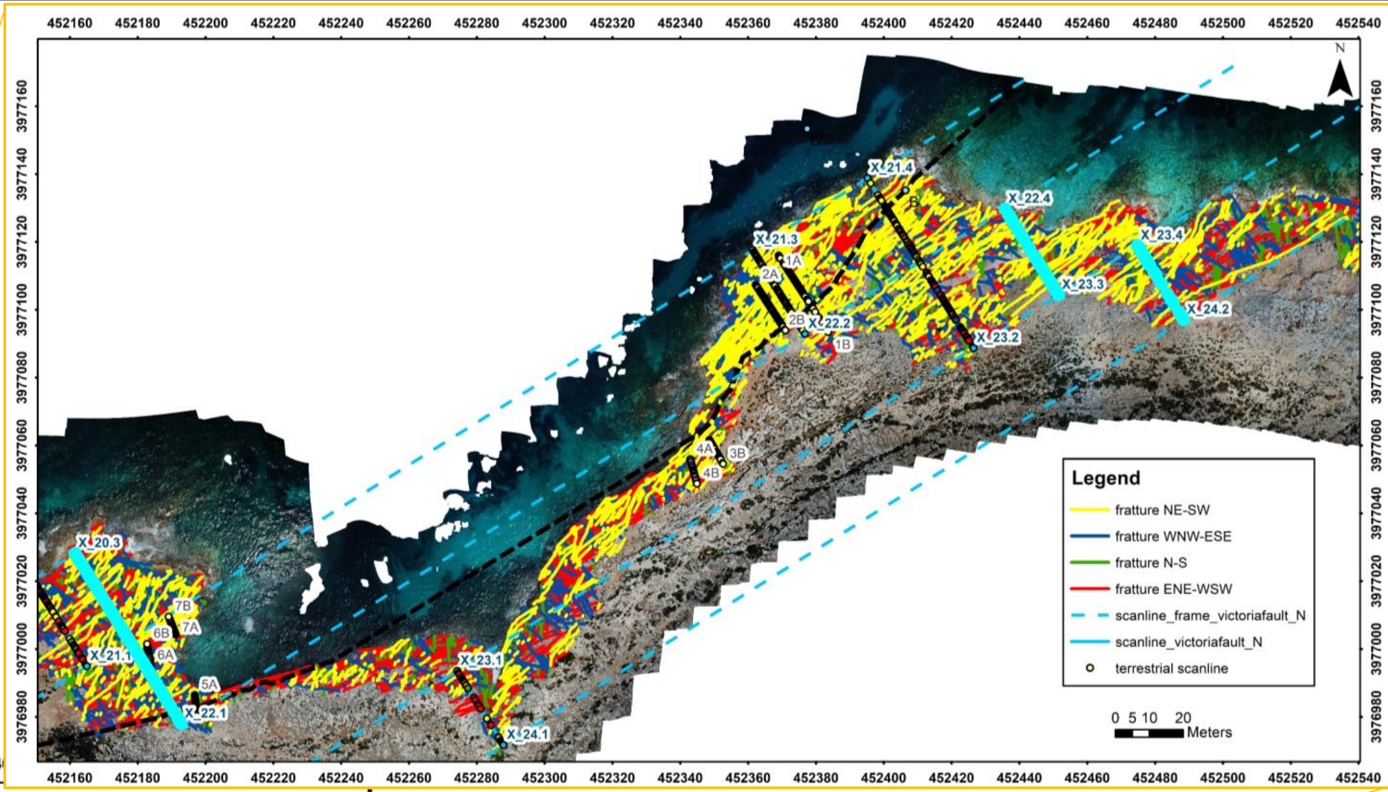

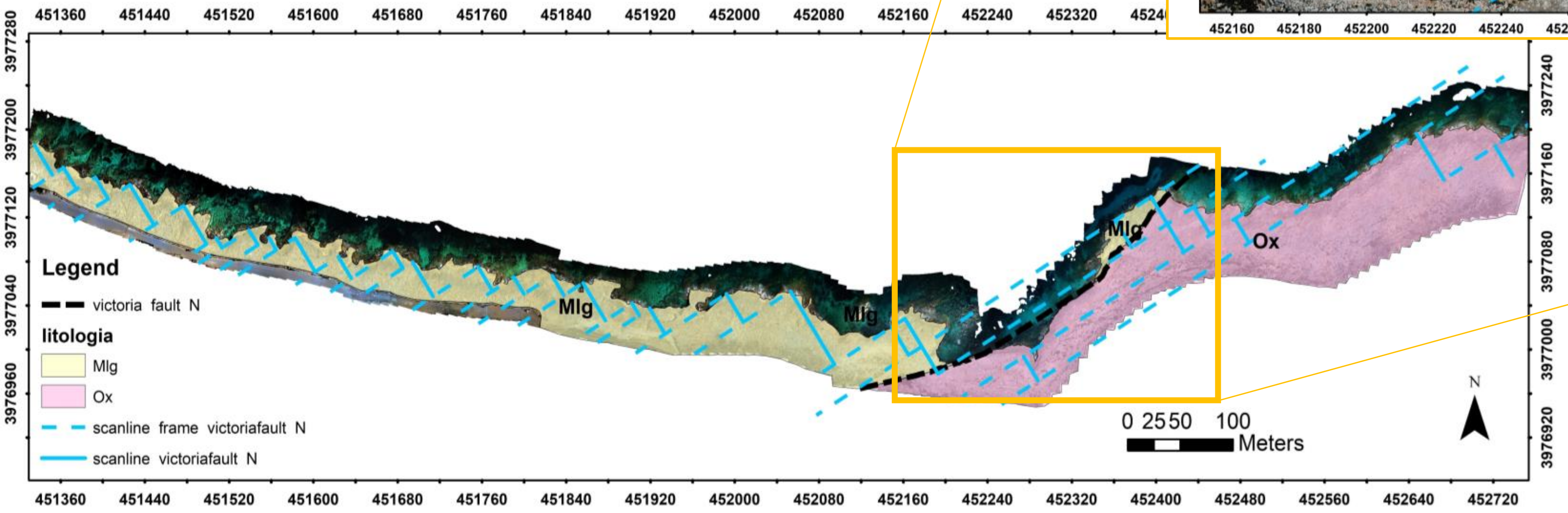

→ calculate the intersections between fracture sets and scanlines

Victoria Fault NE (2)

Two equivalent methods to calculate **progressive distances** along scanlines:

1. Pythagorean theorem and Terzaghi correction (1965)

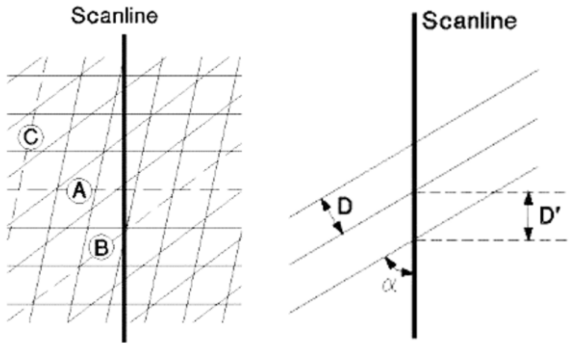

$$W = (1)cosec\alpha$$

2. Calculation of the distance from a point to a plane

$$d(P,\pi) = \frac{|ax_P + by_P + cz_P + d|}{\sqrt{a^2 + b^2 + c^2}}$$

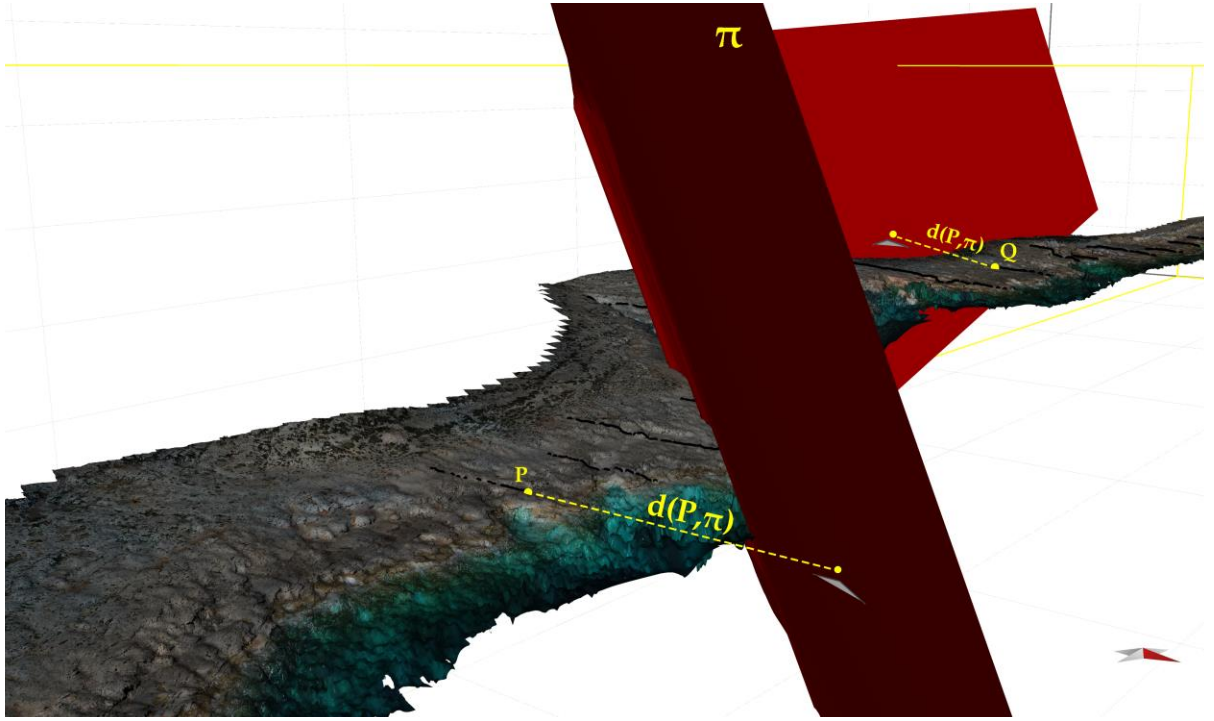

→ statistical analysis of spacing

Geological and structural field analysis

- Orientation statistics of the master fault plane of the Victoria Fault:

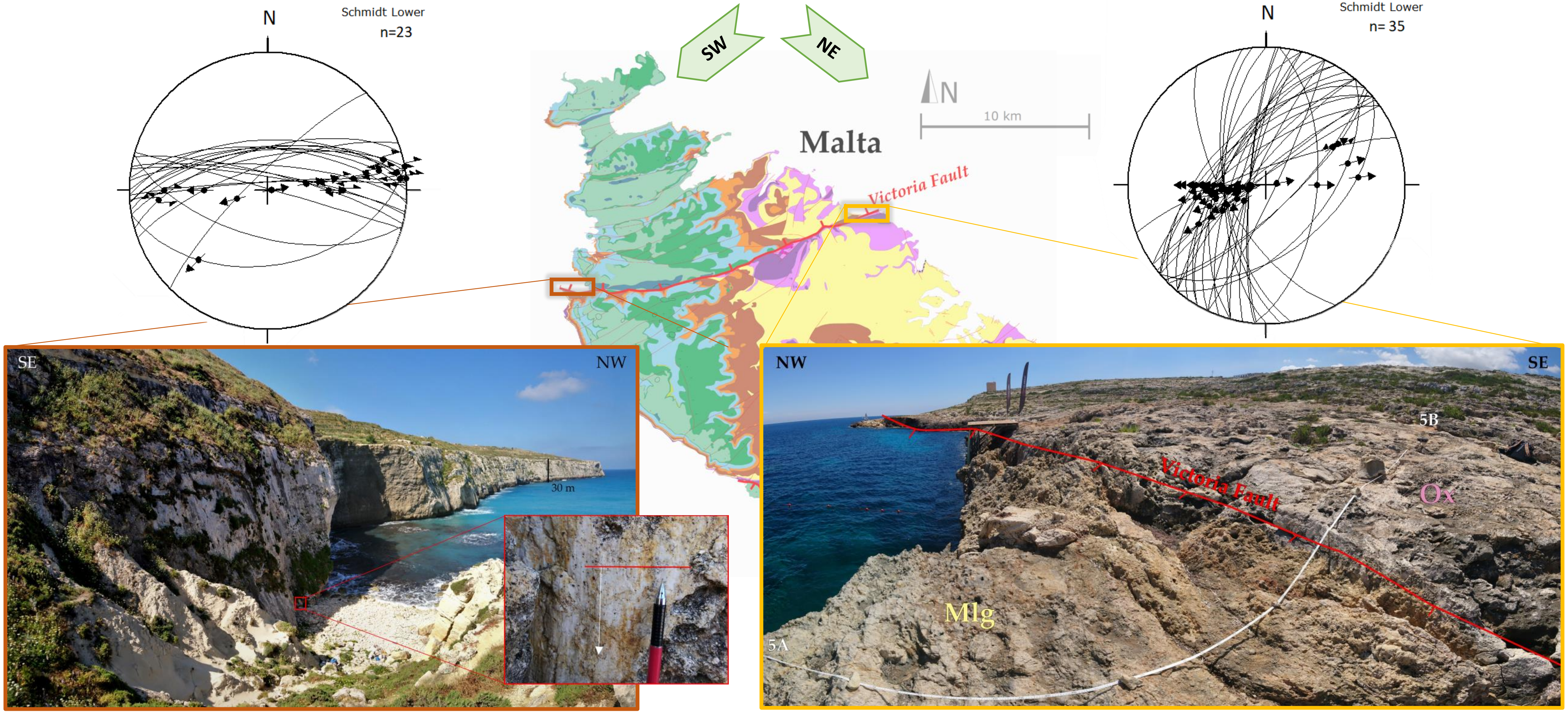

→ results consistent with the N-S extensional phase (D2) of Martinelli et al. (2019)

Photogrammetry fracture analysis

- Orientation statistics of fractures traced on the orthophotos: 4 well-defined sets.

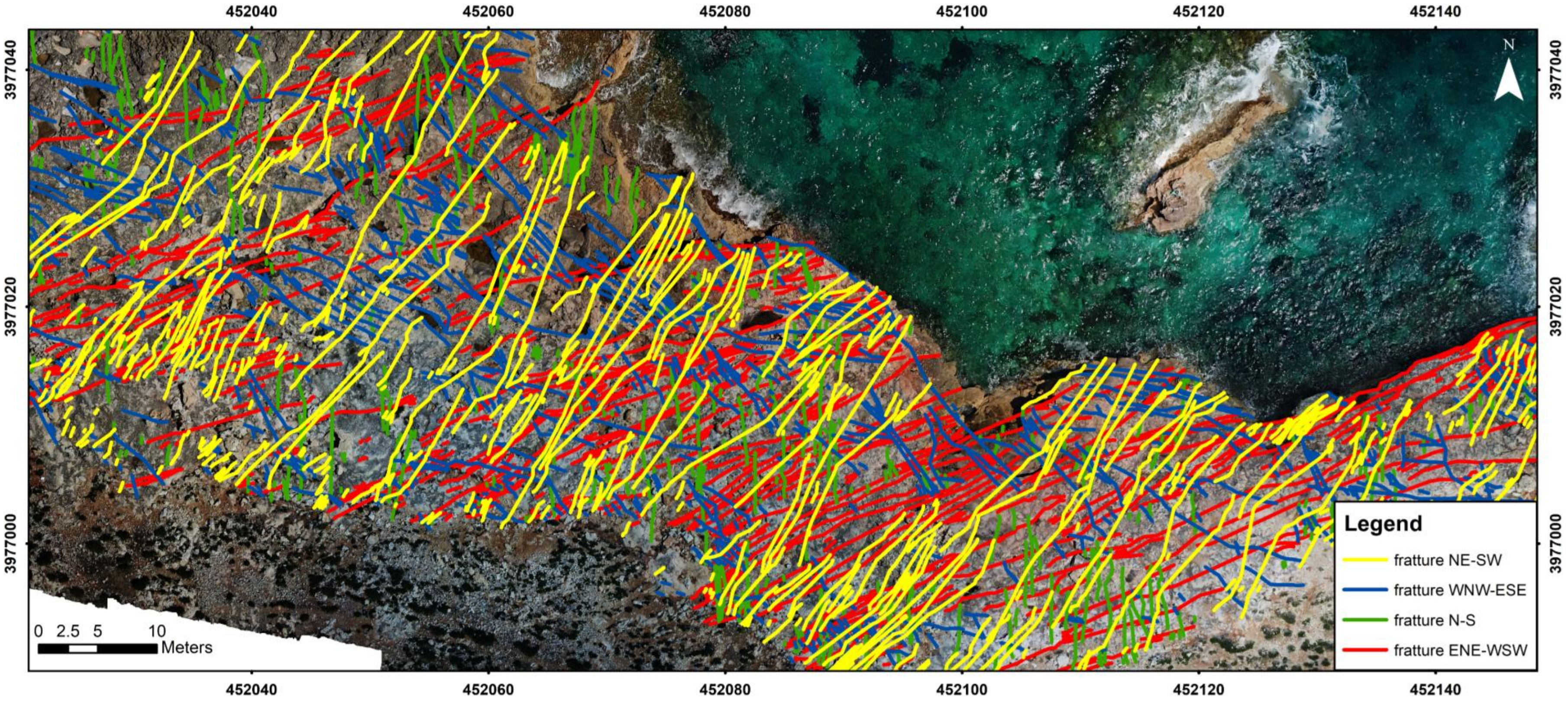

	Fisher Mean Vector				
set	quantity	trend	plunge	kappa	mean lenght
ENE-WSW	2988	64.1	0	1.5	0.3251
NE-SW	4039	35.5	0	2	0.4899
N-S	2100	1.5	0	1.6	0.3598
WNW-ESE	4058	147.4	0	1.2	0.1766

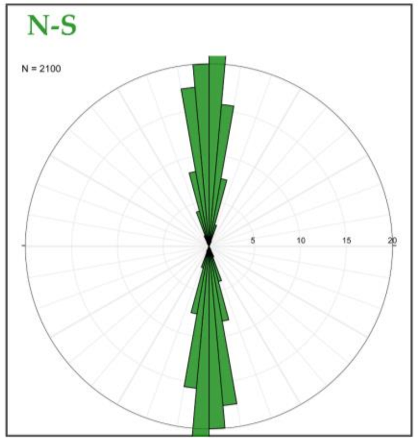

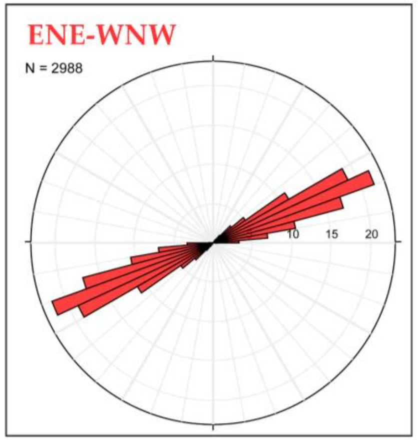

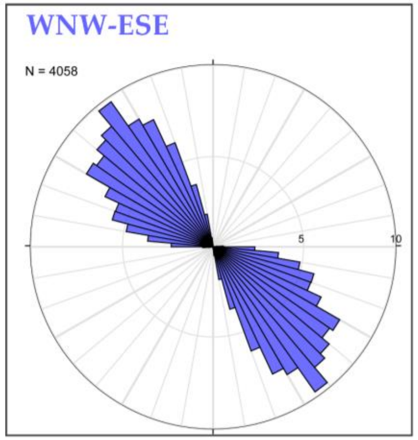

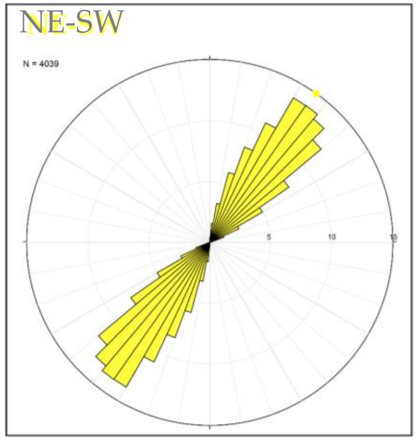

Fracture analysis: lengths

- Fracture length statistics for the 4 sets and for the terrestrial scanlines

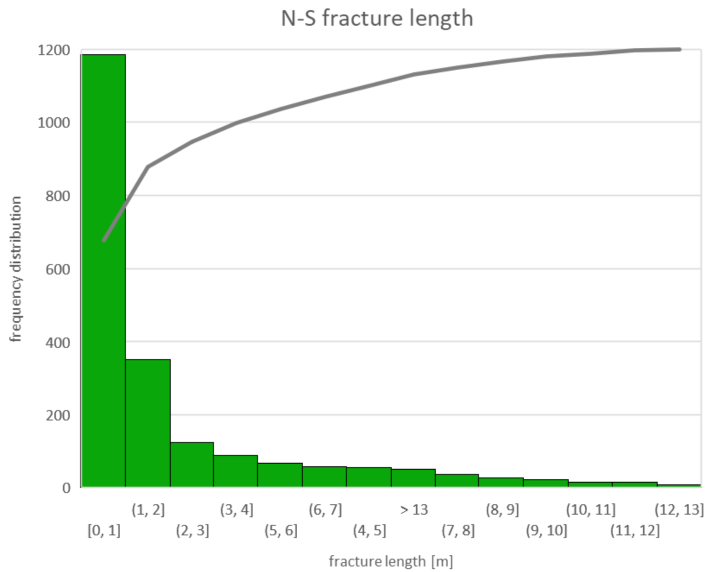

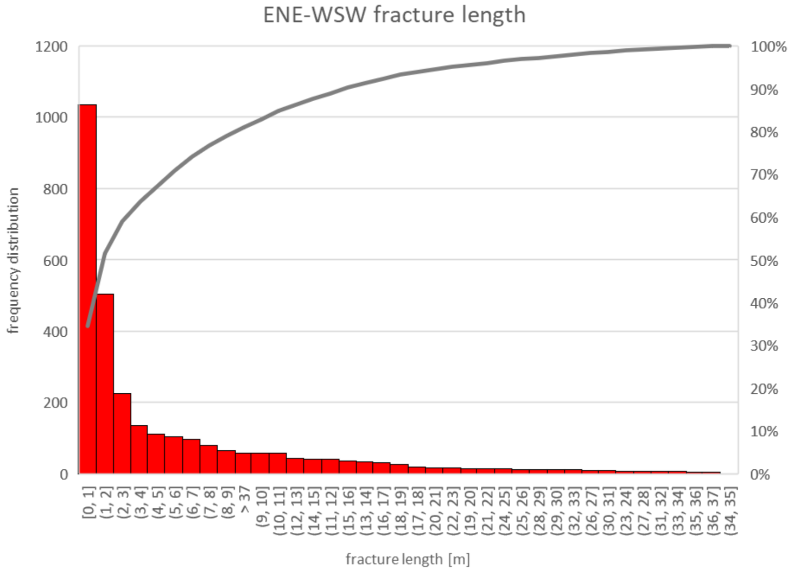

SET statistics	ENE-WNW	NE-SW	N-S	WNW-ESE
Count:	2988	4039	2100	4058
Minimum [m]:	0.109	0.112	0.118	0.136
Maximum [m]:	125.612	74.056	28.845	59.564
Mean [m]:	6.222	3.996	2.309	3.268
Standard Deviation [m]:	10.175	6.288	3.406	4.996

→ negative exponentials

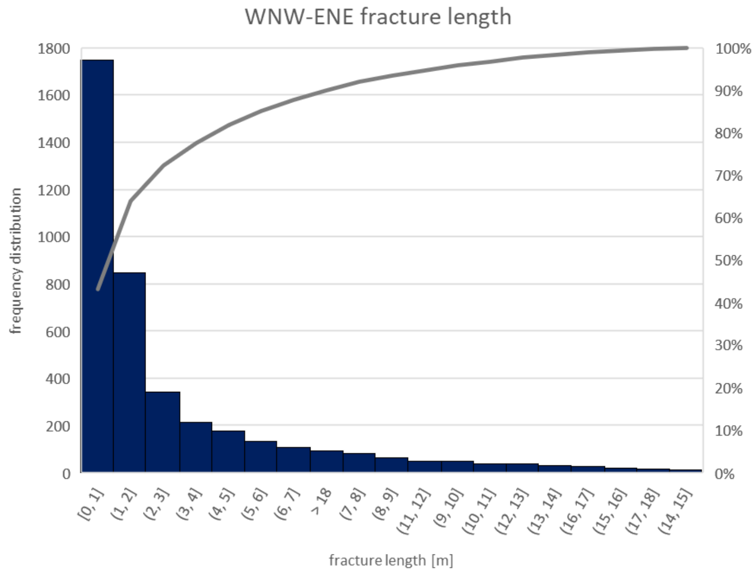

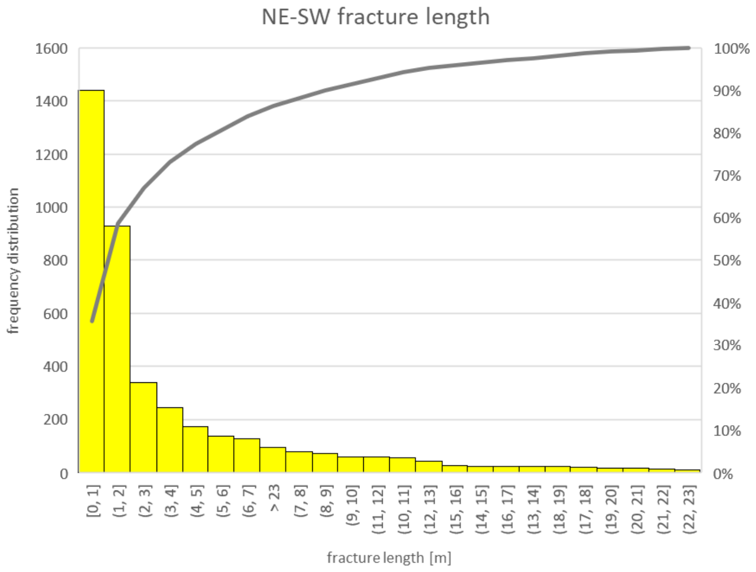

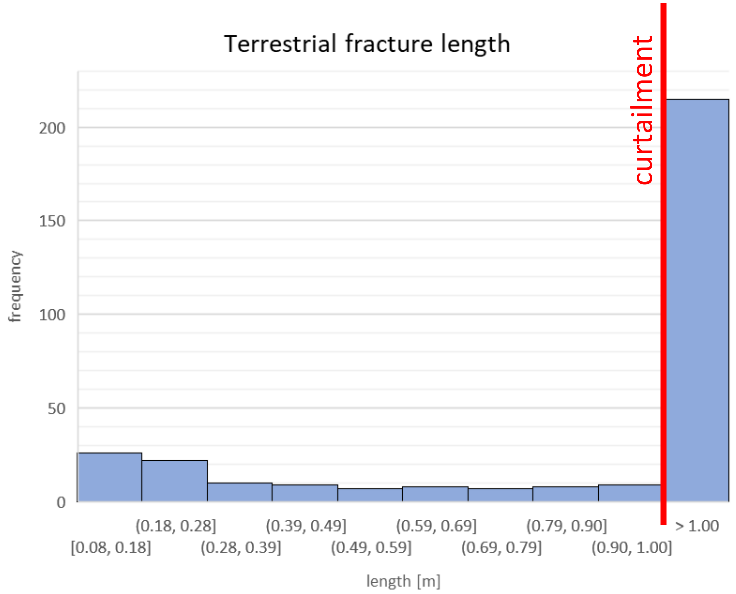

Statistical analysis of field scanlines (1)

Statistical analysis of the spacing (ex. scanline 1):

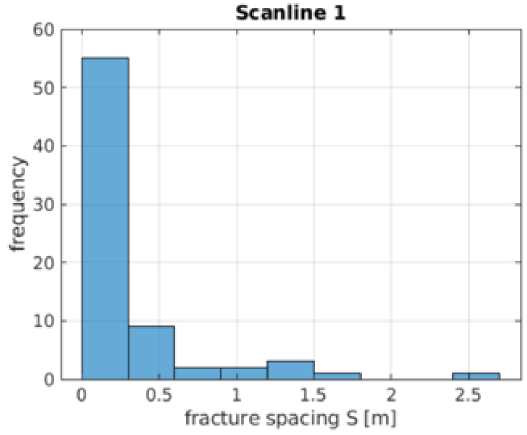

spacing frequency

Spacing statistics: n. data = 74 - mean = 0.32979 - std.dev. = 0.42718 - skewness = 2.903 - kurtosis = 11.9128 - P10 = 3.0322

barcode

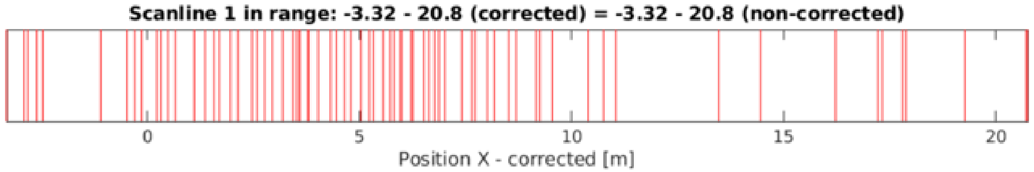

K-S test for uniform spacing

Results of K-S test for UNIFORM fracture spatial distribution with lower bound = -3.3201 and upper bound = 20.7548

K statistics = 0.28981 p-value = 5.3446e-06 Ho = 1

Strong evidence against Ho of no difference with UNIFORM distr. -> Ho rejected -> no UNIFORM fracture distribution is detected at 5% significance

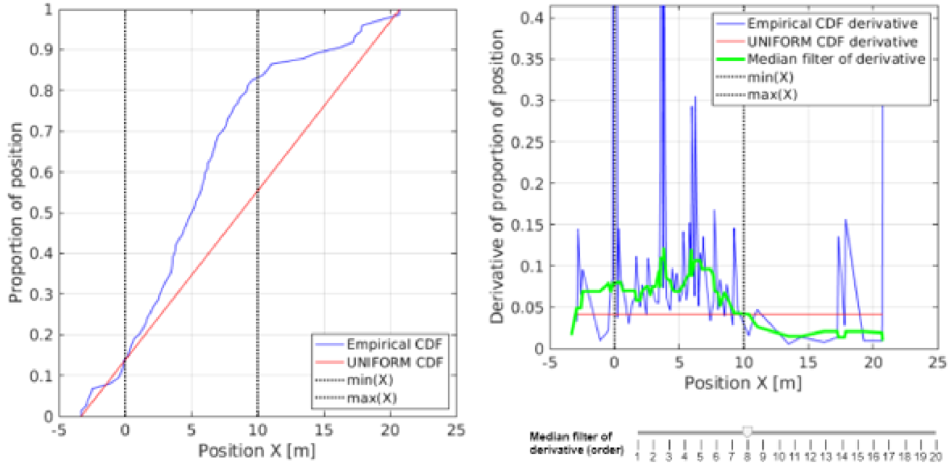

Statistical analysis of field scanlines (1)

Statistical analysis of the spacing (ex. scanline 1):

spacing frequency

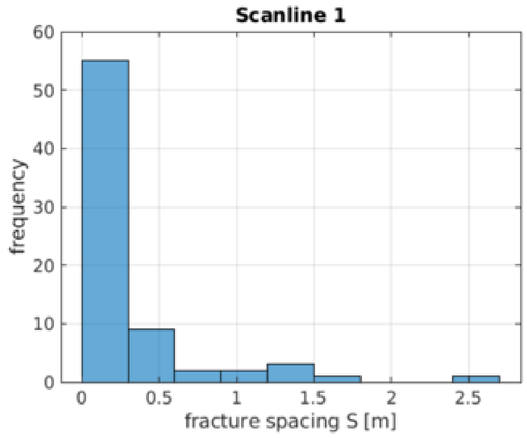

barcode

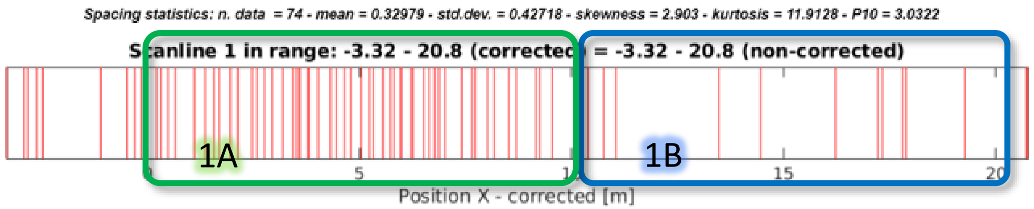

K-S test for stationary spacing

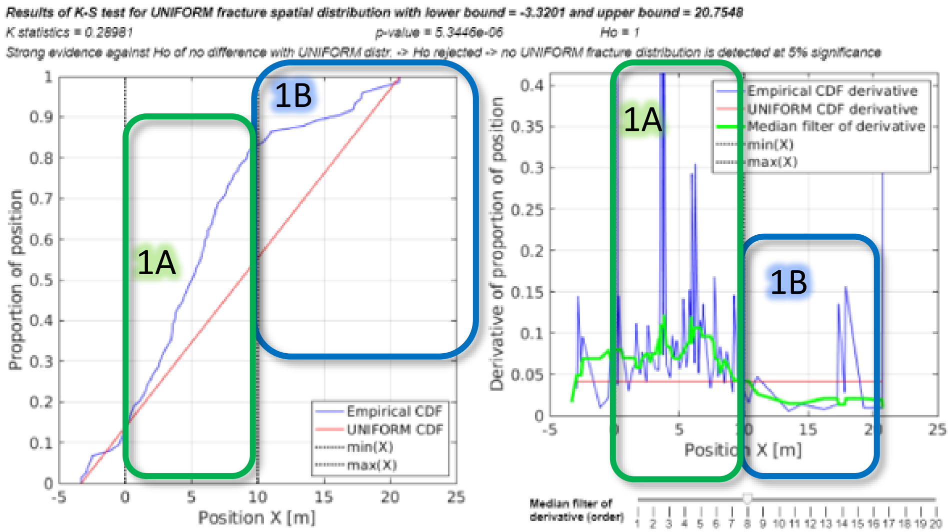

distribution statistics

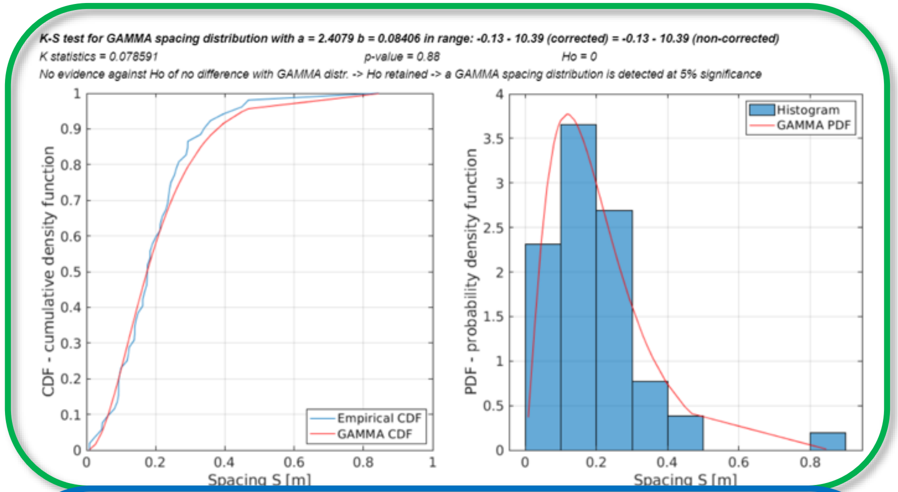

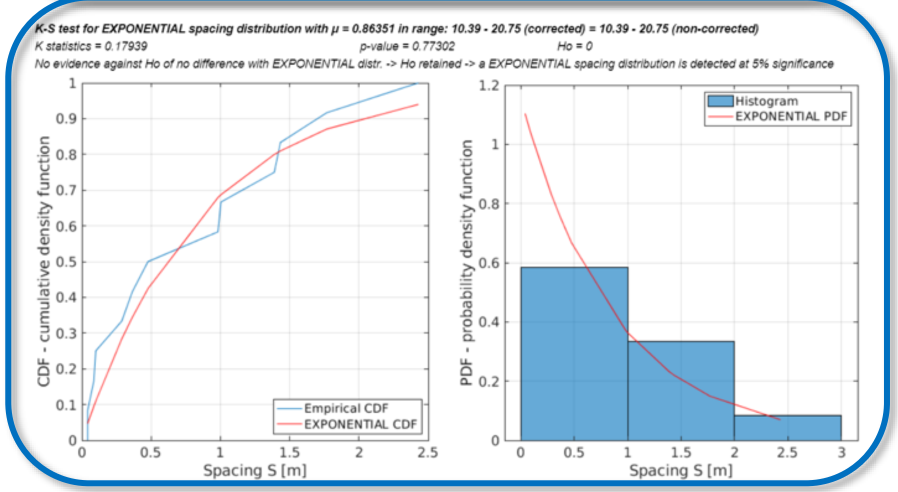

Statistical analysis of field scanlines (2)

TERRESTRIAL SCANLINE						Spatial distribution statistics				Spacing statistics																
method	lithology	scanline	X_min	X_max	n. data	trend test	pattern test	uniform dist. test	Poisson dist. test	scan.	mean	std. dev.	skewness	kurtosis	P_{10}	exponential dist.		Gamma dist.			lognormal dist.			normal dist.		
																μ and σ	p-value	a	b	p-value	μ	σ	p-value	μ	σ	p-value
Terzaghi	mlg	1:0.00-15.50	0	15.5	62	no_trend	no_pattern	retained	retained	1a	0.2541	0.22785	3.3696	17.407	3.9355	rejected		1.9677	0.12913	0.31072	-1.6452	0.78172	0.1438	rejected		
Terzaghi	ox	1:15.5-17	15.5	27	13	no_trend	no_pattern	retained	retained	1b	0.38058	0.32897	0.55061	2.1262	2.6275	0.38058	0.91012	1.0113	0.37632	0.90236	-1.5361	1.3172	0.77493	0.38058	0.32897	0.87707
Terzaghi	mlg	2:0.00-17.2	0	17.2	76	trend	no_pattern	retained	retained	2	0.09108	0.07136	1.8463	7.4887	10.9799	rejected		2.0052	0.045421	0.37619	-2.6657	0.75185	0.52005	0.091075	0.071362	0.057336
Terzaghi	ox	3:0.00-3.14	0	3.14	27	no_trend	no_pattern	retained	retained	3a	0.05328	0.0444	1.7814	5.3296	18.7693	0.05328	0.07661	1.9459	0.027381	0.60885	-3.2107	0.77985	0.79747	0.053278	0.044396	0.10065
Terzaghi	ox	3:3.14-8.10	3.14	8.1	13	no_trend	no_pattern	retained	retained	3b	0.18235	0.13709	1.6582	4.964	5.4841	0.18235	0.07096	2.3445	0.077777	0.57742	-1.93	0.73235	0.37791	0.18235	0.13709	0.27608
Terzaghi	ox	4:0.00-7.6	0	7.6	25	no_trend	no_pattern	retained	retained	4	0.19911	0.16236	0.83854	2.0193	5.0223	0.19911	0.32611	1.7164	0.116	0.35488	-1.9326	0.81721	0.38036	0.19911	0.16236	0.10168
Terzaghi	mlg	5:0.00-1.60	0	1.6	24	no_trend	no_pattern	retained	retained	5a	0.05151	0.03338	0.60767	2.313	19.4129	0.05151	0.24512	2.2227	0.023175	0.85337	-3.2074	0.76424	0.83506	0.051512	0.033376	0.88843
Terzaghi	ox	5:1.60-6.60	1.6	6.6	15	no_trend	no_pattern	retained	retained	5b	0.26446	0.10776	-0.75436	2.6021	3.7813	rejected		4.0289	0.065641	0.22827	-1.4593	0.60825	0.13347	0.26446	0.10776	0.65857
Terzaghi	mlg	6:0.00-6.3	0	6.3	33	no_trend	no_pattern	retained	retained	6	0.13748	0.11308	1.1087	3.9128	7.2736	0.13748	0.42347	1.3547	0.10149	0.60904	-2.3967	1.0353	0.25983	0.13748	0.11308	0.59243
Terzaghi	mlg	7:0.00-5.8	0	5.8	30	trend	no_pattern	retained	retained	7	0.11047	0.07513	1.5068	5.3681	9.0524	rejected		2.2617	0.048843	0.88228	-2.4401	0.78815	0.54175	0.11047	0.075126	0.31023

Depending on the distance from the fault, we observe 3 distributions (from the closest) with different skewness:

- normal
- log-normal
- exponential

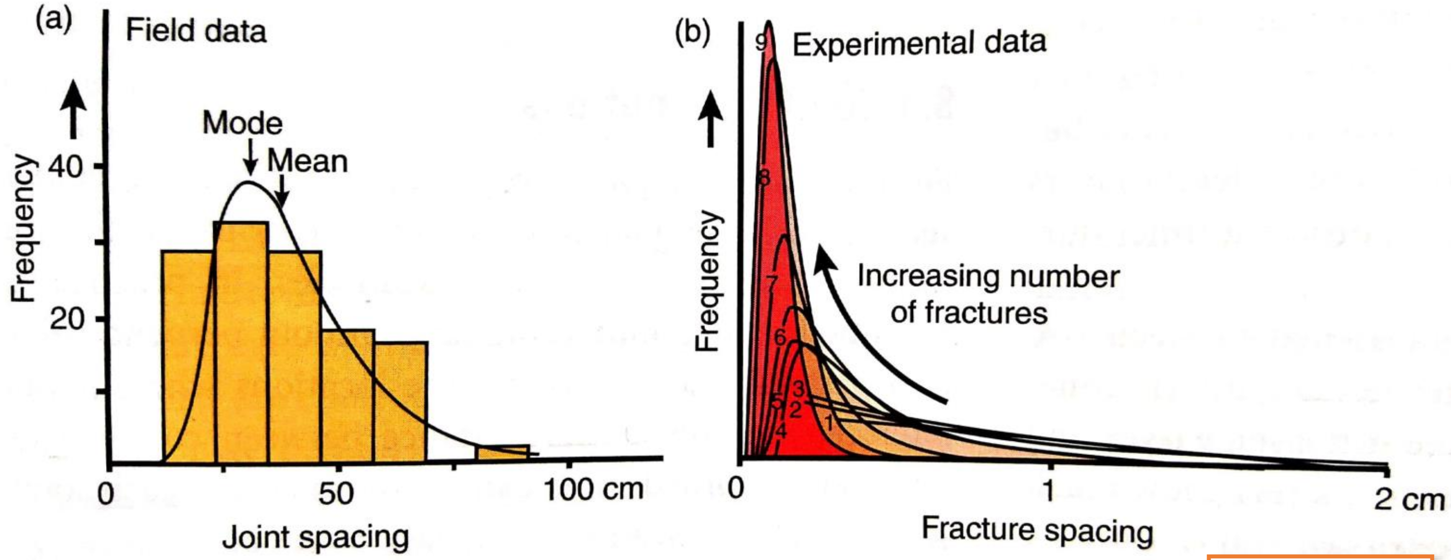

Fossen (2016)

Statistical analysis of (merged) scanline from photogrammetry (1)

SCANLINE VICTORIA FAULT							Spatial distribution statistics				Spacing statistics															
lithology	scanline		main scanline	X_min	X_max	n. data	trend test	pattern test	uniform dist. test	Poisson dist. test	mean	std. dev.	skewness	kurtosis	P10	exponential dist.		Gamma dist.			lognormal dist.			normal dist.		
	start	end														μ and σ	p-value	a	b	p-value	μ	σ	p-value	μ	σ	p-value
mlg	X_0.0	X_2.1	1	-563.84	-512.4	75	no_trend	no_pattern	retained	retained	0.6951	0.56414	2.2524	10.862	1.4386	0.6951	0.097651	1.8087	0.38431	0.81434	-0.66492	0.83296	0.48041	rejected		
mlg	X_2.2	X_4.1	1	-510.57	-450.52	47	no_trend	pattern	retained	retained	1.3054	1.0095	1.2194	4.1784	0.76607	1.3054	0.23981	1.6462	0.79294	0.81881	-0.067006	0.91367	0.66111	1.3054	1.0095	0.055785
mlg	X_4.2	X_5.1	1	-447.49	-410.31	44	no_trend	no_pattern	retained	retained	0.86454	0.5996	1.0966	3.5776	1.1567	rejected		2.1497	0.40217	0.70741	-0.39583	0.7644	0.82841	0.86454	0.5996	0.17034
mlg	X_5.2	X_6.1	1	-409.06	-400.46	15	no_trend	no_pattern	retained	retained	0.61384	0.55263	0.41536	1.6368	1.6291	0.61384	0.55877	0.95001	0.64614	0.62669	-1.0993	1.2998	0.64707	0.61384	0.55263	0.62778
mlg	X_6.2	X_7.1	1	-398.57	-385.28	10	no_trend	no_pattern	retained	retained	1.4766	1.0604	0.67944	2.1364	0.67721	1.4766	0.69968	2.1701	0.68045	0.83444	0.14202	0.76778	0.95949	1.4766	1.0604	0.59382
mlg	X_7.2	X_11.1	1	-383.13	-301.11	93	no_trend	no_pattern	retained	retained	0.89155	0.79469	1.3776	4.6219	1.1216	0.89155	0.70964	1.2818	0.69552	0.95278	-0.55308	1.0348	0.67238	rejected		
mlg	X_11.2	X_15.1	1	-297.43	-204.88	82	no_trend	no_pattern	retained	retained	1.1426	0.97363	1.8332	7.1381	0.87518	rejected		1.6684	0.68487	0.61679	-0.19537	0.85494	0.62005	rejected		
mlg	X_15.2	X_17.1	1	-203.28	-155.54	69	no_trend	no_pattern	retained	retained	0.70196	0.64434	1.7542	6.4307	1.4246	0.70196	0.52685	1.3188	0.53226	0.92626	-0.77866	1.0128	0.76063	rejected		
mlg	X_17.2	X_19.1	1	-154.46	-104.15	58	no_trend	no_pattern	retained	retained	0.88259	0.87516	1.8564	6.2161	1.133	0.88259	0.84288	1.2182	0.7245	0.87143	-0.58848	1.0499	0.7926	0.88259	0.87516	0.053061
mlg	X_19.2	X_20.1	1	-100.54	-33.04	111	trend	no_pattern	rejected	retained	0.61362	0.59063	2.5834	11.351	1.6297	0.61362	0.097139	1.4842	0.41342	0.63845	-0.86163	0.90676	0.46237	rejected		
mlg	X_20.2	X_21.1	1	-31.46	-5.89	53	trend	no_pattern	rejected	retained	0.49164	0.468	1.9739	7.7566	2.034	0.49164	0.65624	1.3679	0.35942	0.67454	-1.1181	0.95787	0.90237	0.49164	0.468	0.072445
mlg/ox	X_20.3	X_22.1	1	-32.07	19.98	123	no_trend	no_pattern	retained	retained	0.42668	0.34777	1.4815	5.6531	2.3437	0.42668	0.053169	1.5485	0.27554	0.99306	-1.2081	0.92711	0.75738	rejected		
ox	X_23.1	X_24.1	0	48.64	70.74	22	no_trend	no_pattern	retained	retained	1.0526	1.0837	1.5069	3.9497	0.95007	1.0526	0.79409	1.2805	0.82199	0.64632	-0.38758	0.95628	0.95897	1.0526	1.0837	0.08243
mlg/ox	X_21.3	X_22.2	0	-7.73	16.89	74	no_trend	no_pattern	retained	retained	0.33716	0.24261	1.276	4.6283	2.966	0.33716	0.054613	2.0189	0.167	0.94883	-1.3549	0.78335	0.87896	0.33716	0.24261	0.097448
mlg/ox	X_21.4	X_23.2	0	0.33	44.31	99	no_trend	no_pattern	retained	rejected	0.44874	0.41898	2.2294	9.1668	2.2285	0.44874	0.10223	1.5001	0.29914	0.49982	-1.1703	0.89387	0.64906	rejected		
ox	X_22.4	X_23.3	1	20.12	43.42	39	no_trend	no_pattern	retained	retained	0.61305	0.60628	1.5206	4.7755	1.6312	0.61305	0.98049	1.0986	0.55804	0.90976	-1.0091	1.1493	0.8162	0.61305	0.60628	0.098845
ox	X_23.4	X_24.2	1	45.07	67.1	34	no_trend	no_pattern	rejected	retained	0.66751	0.79571	1.9198	5.9402	1.4981	0.66751	0.39283	0.99743	0.66922	0.39481	-0.98308	1.1124	0.97662	rejected		
ox	X_24.3	X_26.1	1	66	136.57	72	no_trend	no_pattern	retained	retained	0.99393	0.93144	1.5258	4.9142	1.0061	0.99393	0.62677	1.2752	0.77944	0.64303	-0.44689	1.0117	0.78848	rejected		

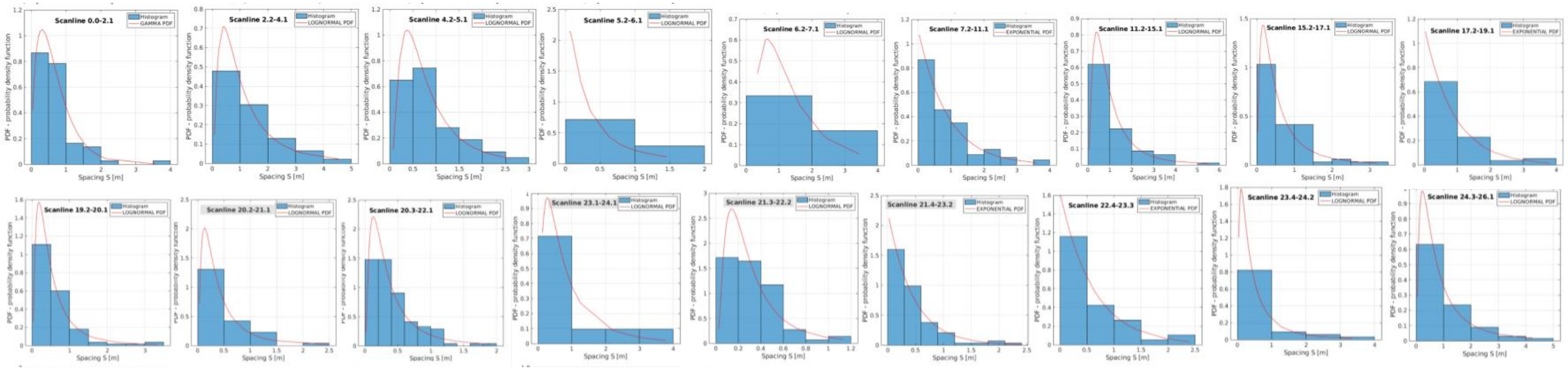

log-normal and exponential distributions

- majority of log-normal distributions

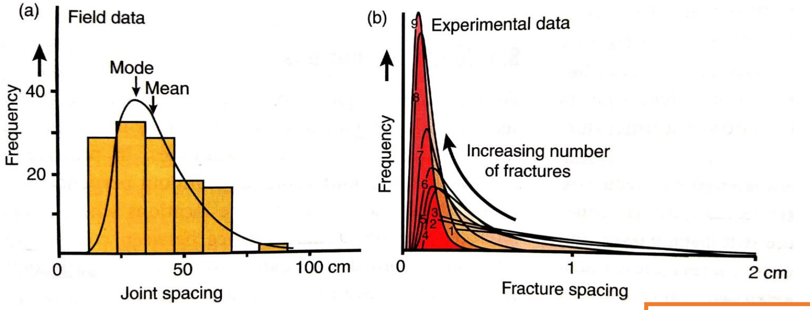

Fossen (2016)

Statistical analysis of the scanline from photogrammetry (2)

- comparison between P_{10} values and the barcode plot: main scanline and secondary scanlines

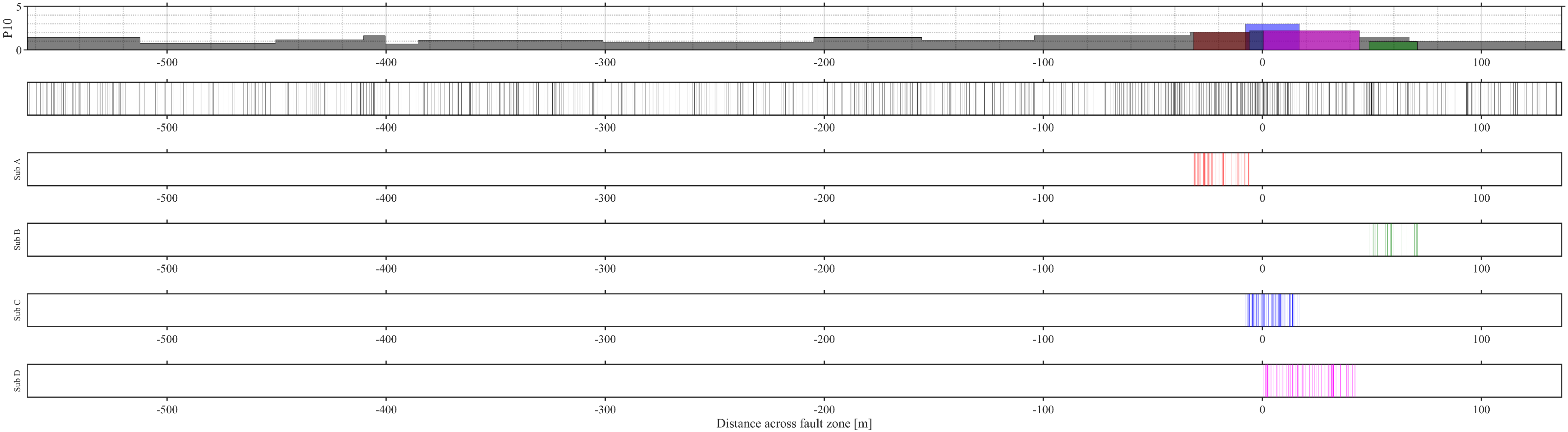

→ the main scanline is representative and consistent with smaller “check” scanlines

→ P_{10} values are higher for Middle Globigerina than for Lower Coralline

→ width of the *inner damage zone*: 120 m

→ presence of *fracture corridors* at -200 and -400 m from the *fault core* (0 m) in the Middle Globigerina

Statistical analysis of the scanline from photogrammetry (3)

- comparison between **P_{10}** values and the barcode plots of field scanlines with those from photogrammetry

field scanlines have higher P_{10} values

but

different detection **scale**:

drone

field

0.10 - 130 m

0.01 - 1 m

so

→ the P_{10} values must be accompanied with the scale of the observed fractures and resolution of the analysis!

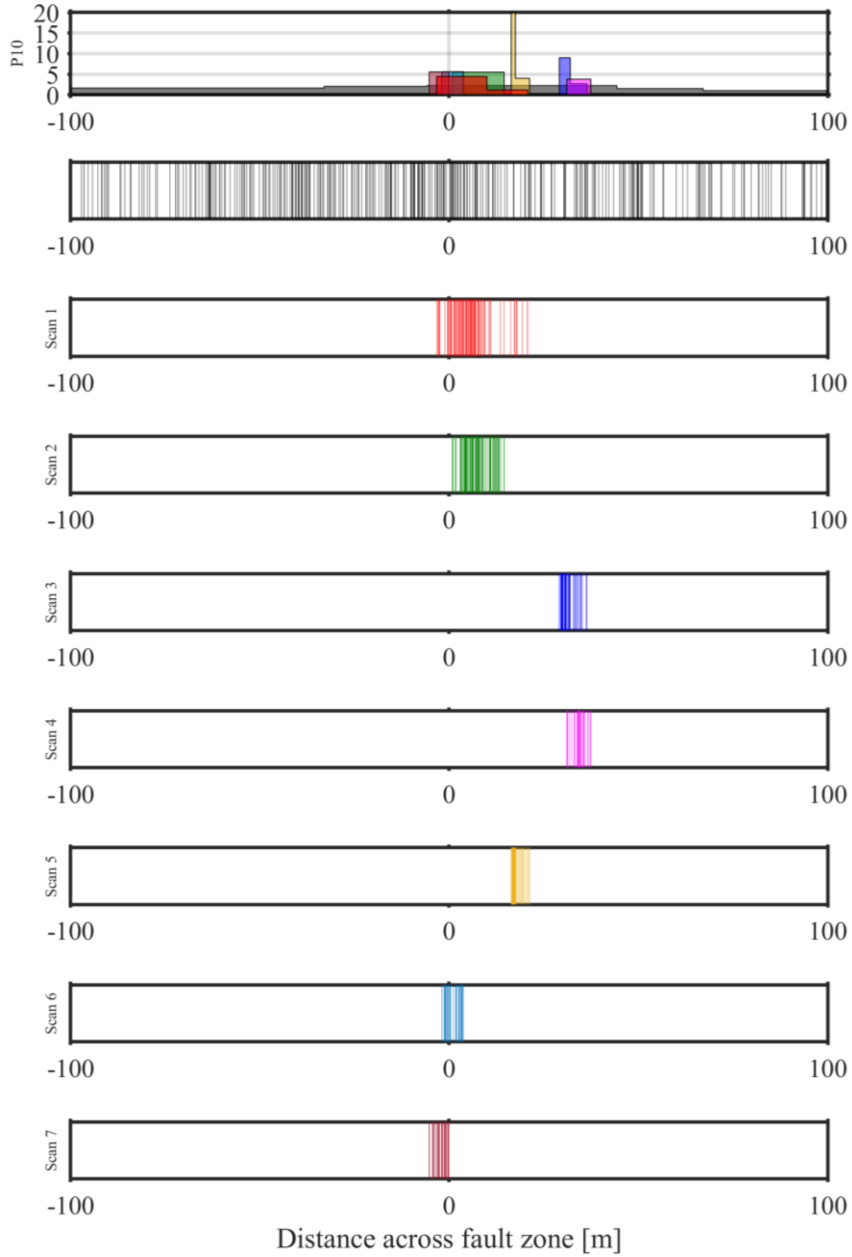

Fracture network analysis (1)

Crosscutting e *abutting* relations between set A and B

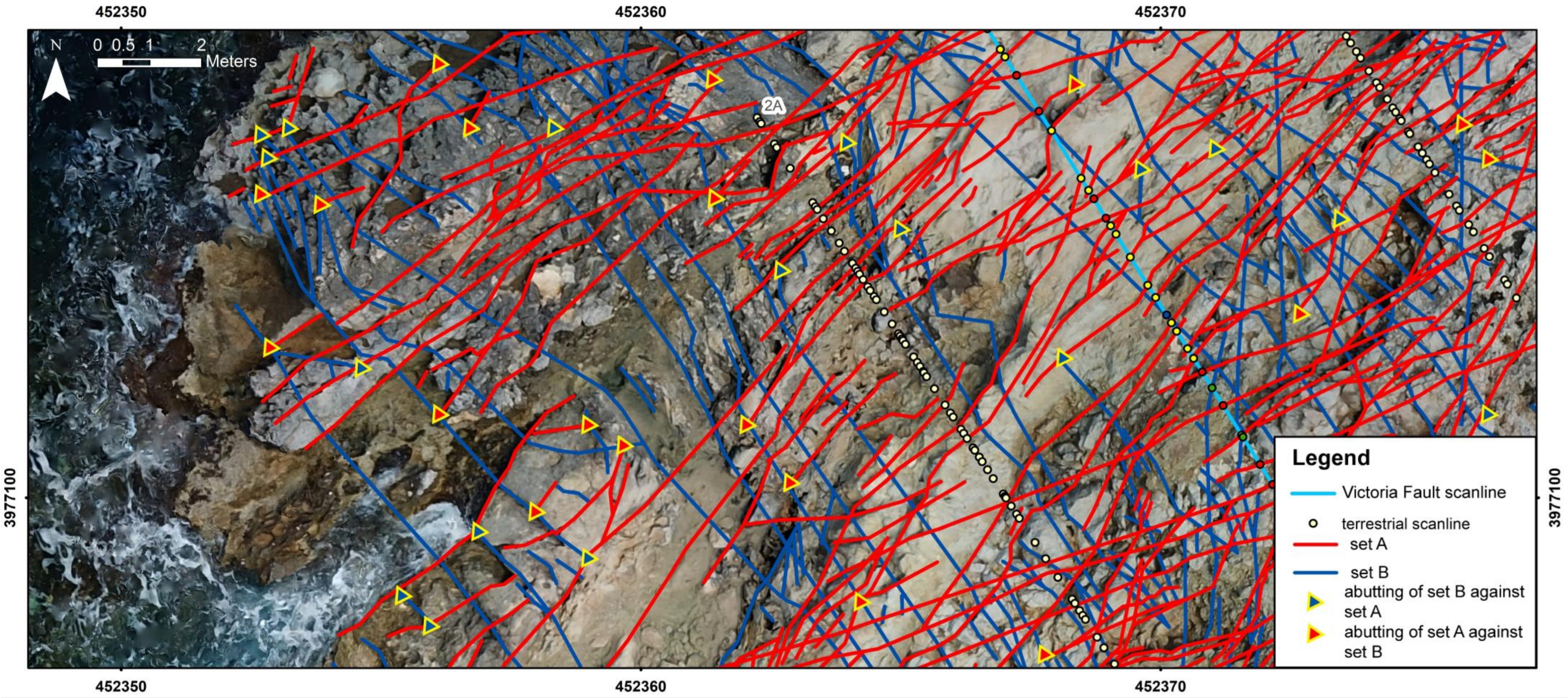

→ both sets are **coeval** and belong to the deformation phase **D2**

Statistical analysis of the scanline from photogrammetry (4)

subdivision into **2 sets**

set A — NE-SW and ENE-WSW — A — main fractures sub-parallel to the Victoria Fault, average spacing 0.98 m

set B — N-S and WNW-ESE — B — secondary fractures, average spacing 3.17 m

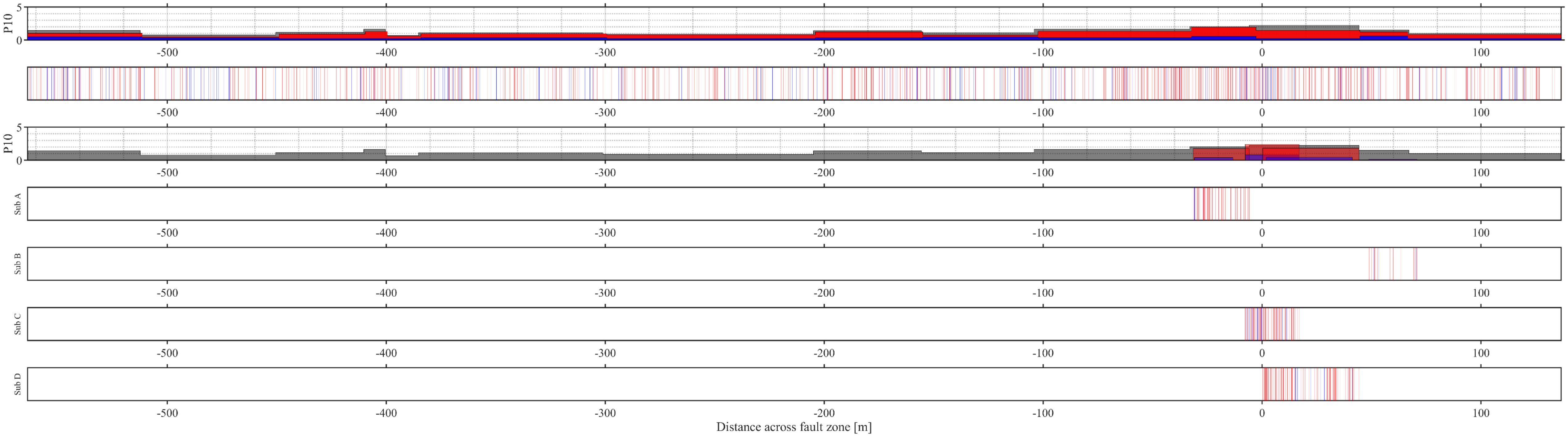

→ set A: greater variability

→ set B: much more stable

Fracture network analysis (2)

deformation evolution based on spacing distributions (e.g. according to Rives et al. 1992):

negative exponential (initial phase) → log-normal (intermediate phase) → normal (final phase)

increasing deformation →

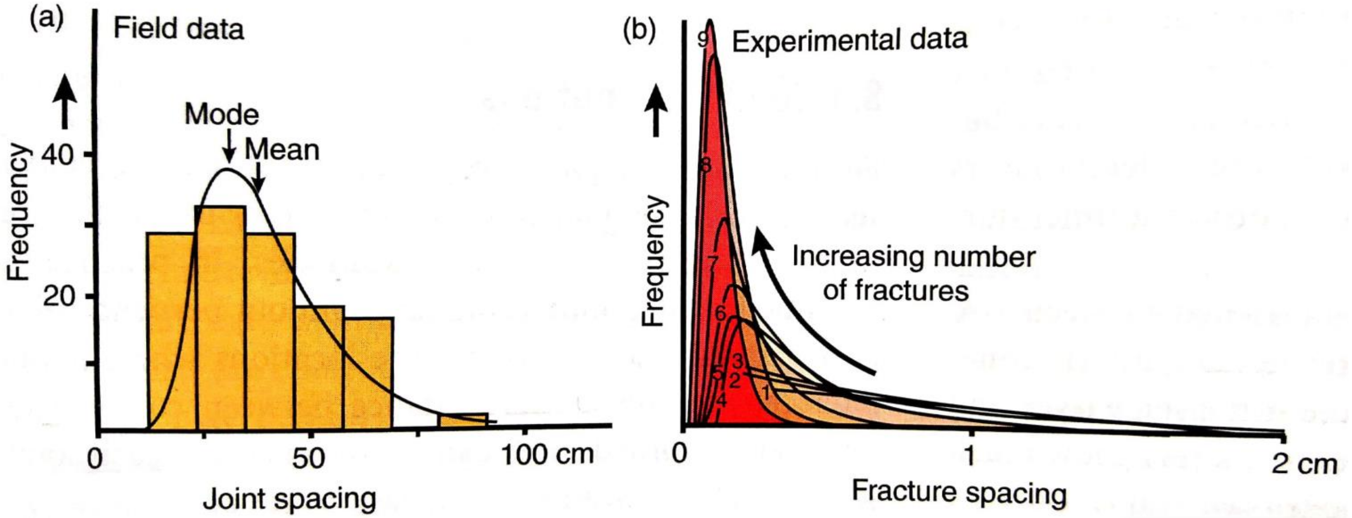

Fossen (2016)

- photogrammetry scanline: majority of log-normal
- field scanline: the three phases are observed according to the distance from the Victoria Fault

Fracture network analysis (3)

analysis of the «maturity» stage of fracturing using the mode/mean ratio (Rives et al., 1992)

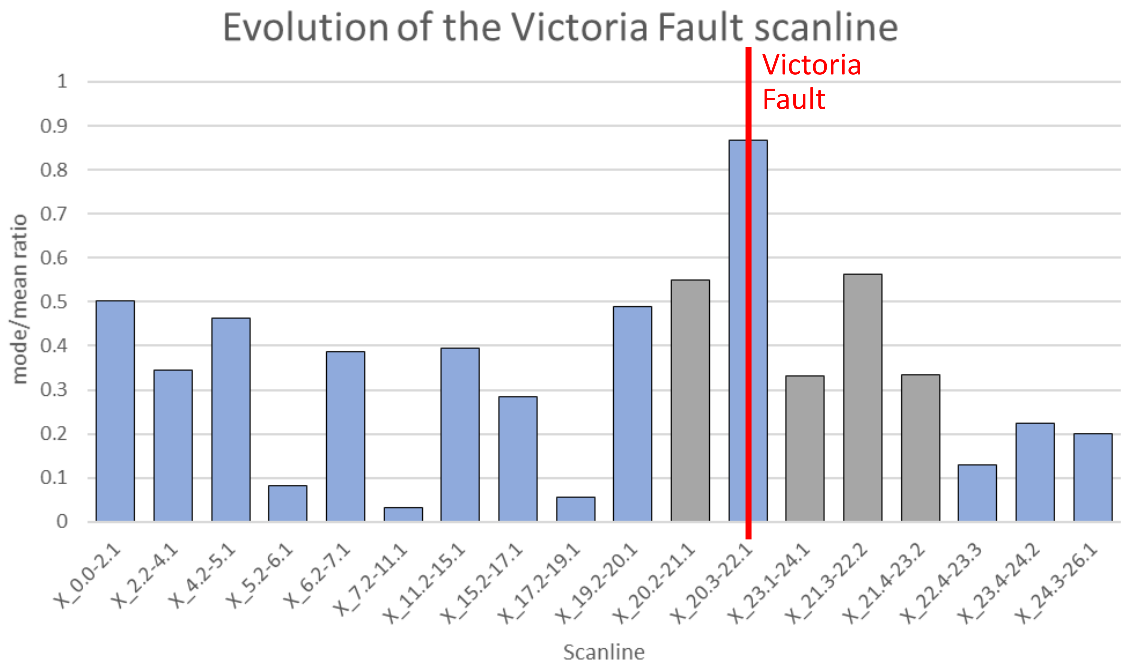

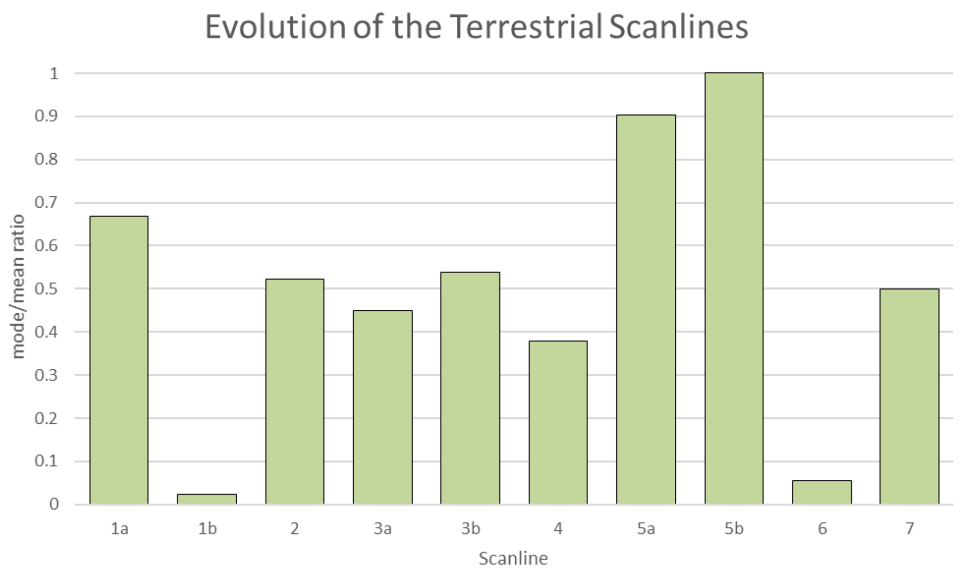

- values → 1 indicate saturation
- values → 0 poorly developed set

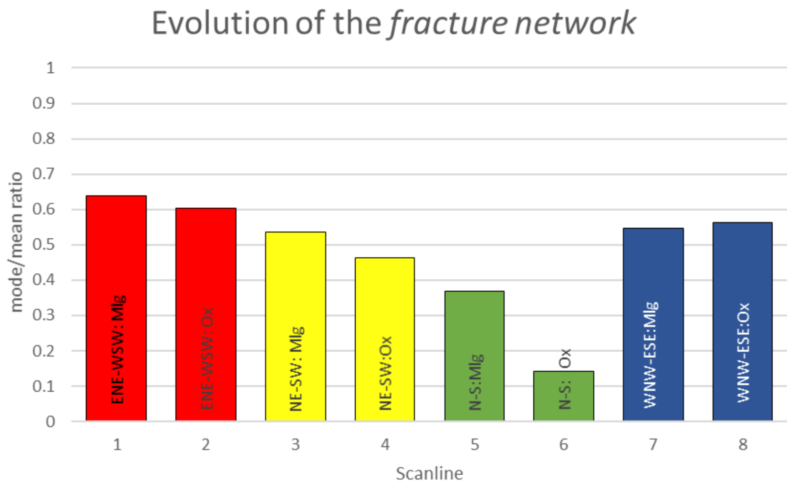

Conclusions (1)

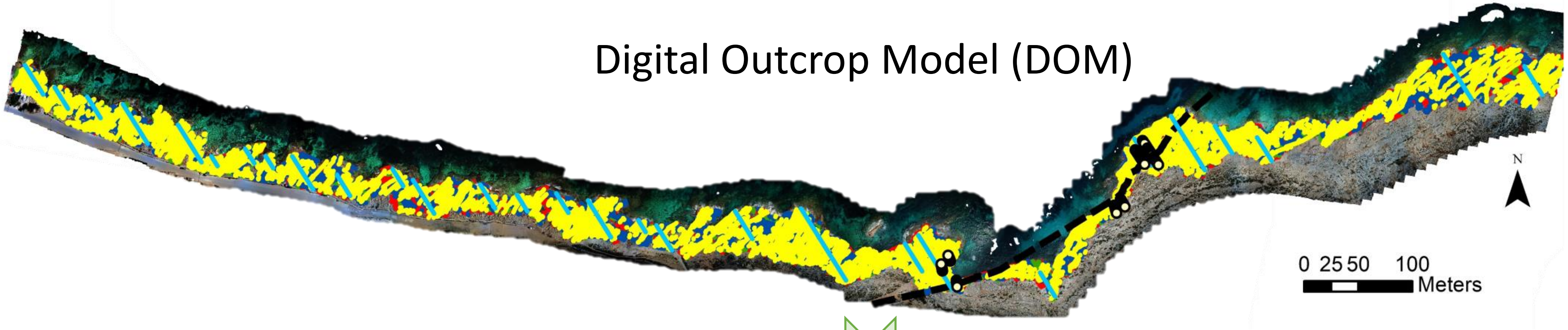

4 sets of fracture:

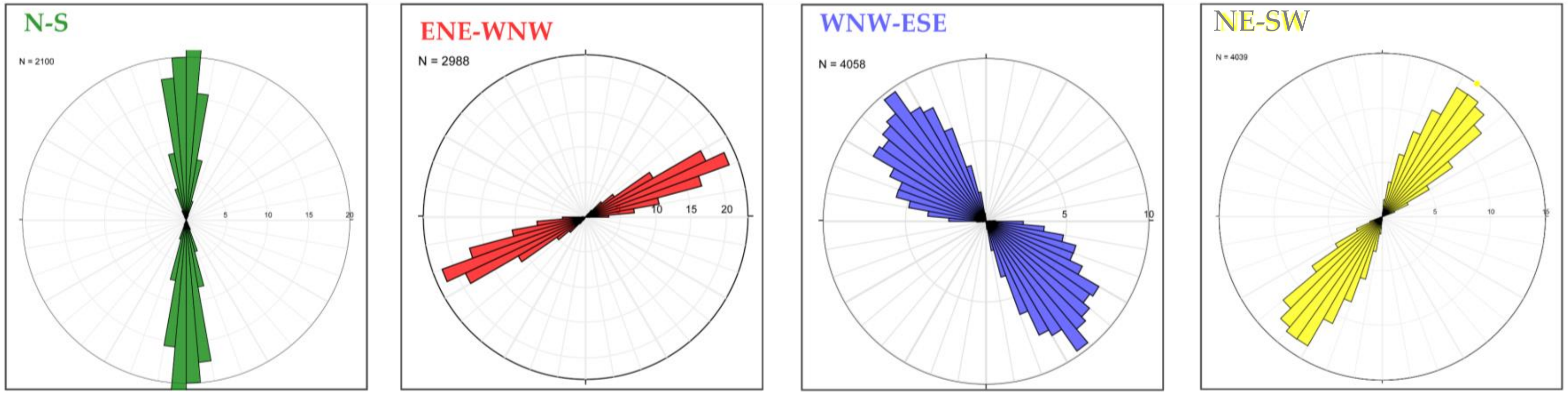

medium spacing:	2.84 m	0.81 m	1.45 m	1.10 m

→ always considering the survey **scale**

Conclusions (2)

«maturity» of the fault zone as described by fracture statistics

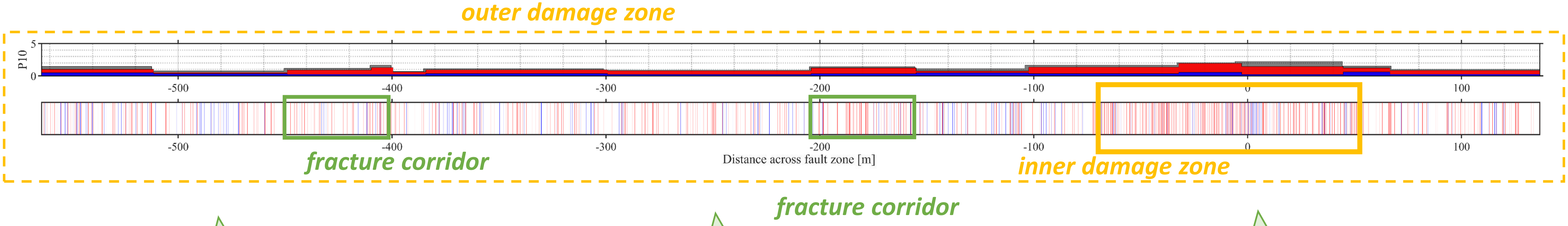

3 — **exponential** distribution

2 — **log-normal** distribution

1 — **normal** distribution

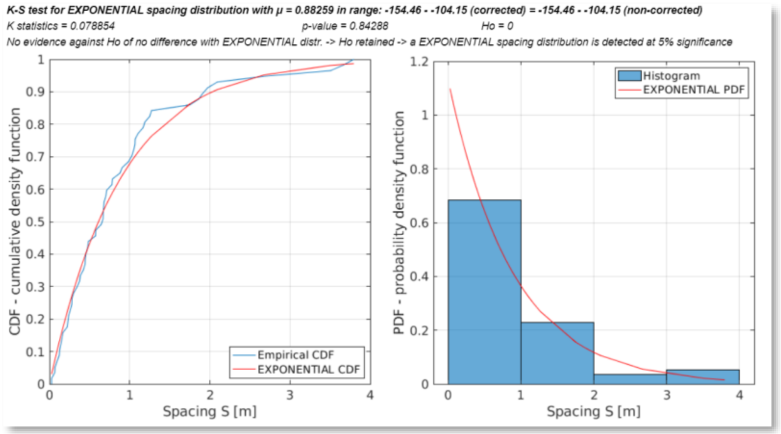

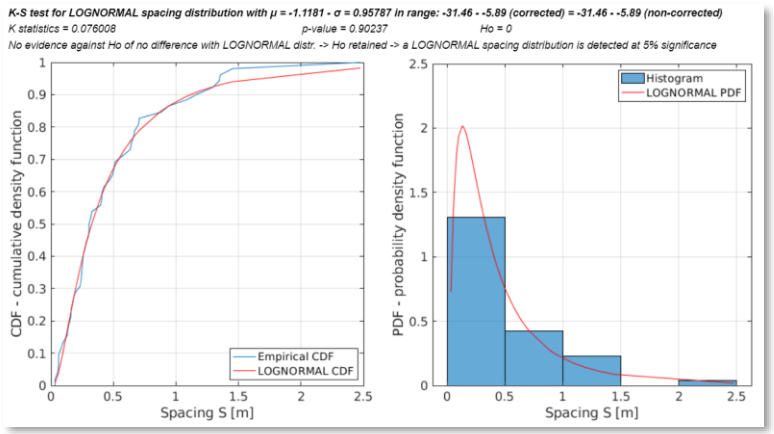

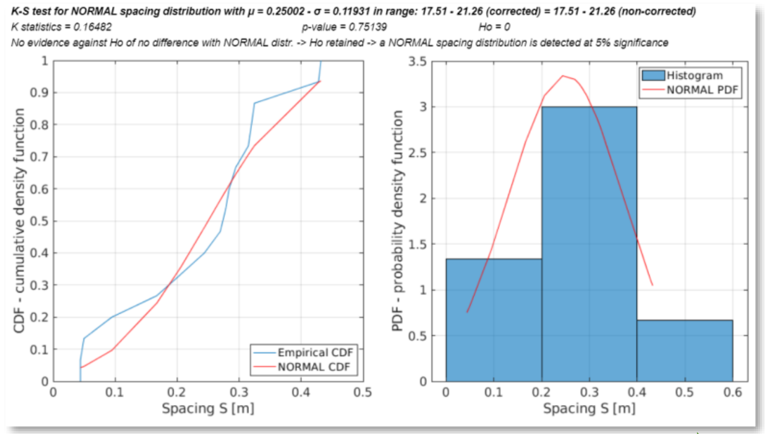

increasing fracture saturation and fault zone maturity

EGU General Assembly 2020
Online | 4–8 May 2020

UNIVERSITA' DEGLI STUDI DI MILANO BICOCCA

Address to:

Università degli Studi di Milano Bicocca, Dipartimento di Scienze dell'Ambiente e della Terra, Milano, Italy

Anna LOSA a.losa3@campus.unimib.it

Andrea BISTACCHI andrea.bistacchi@unimib.it

Mattia MARTINELLI m.martinelli34@campus.unimib.it

References:

Martinelli, M., Bistacchi, A., Balsamo, F., & Meda, M. (2019). *Late Oligocene to Pliocene Extension in the Maltese Islands and Implications for Geodynamics of the Pantelleria Rift and Pelagian Platform*. Tectonics, 38(9), 3394–3415. https://doi.org/10.1029/2019TC005627

Rives, T., Razack, M., Petit, J. P., & Rawnsley, K. D. (1992). *Joint spacing: analogue and numerical simulations.* Journal of Structural Geology, 14(8), 952–937.